university of groningen

University Medical Center Groningen

University of Groningen

The sound of high winds

van den Berg, G.P.

IMPORTANT NOTE: You are advised to consult the publisher's version (publisher's PDF) if you wish to cite from it. Please check the document version below.

Document Version
Publisher's PDF, also known as Version of record

Publication date:
2006

Link to publication in University of Groningen/UMCG research database

Citation for published version (APA):
van den Berg, G. P. (2006). *The sound of high winds: The effect of atmospheric stability on wind turbine sound and microphone noise*. s.n.

Copyright
Other than for strictly personal use, it is not permitted to download or to forward/distribute the text or part of it without the consent of the author(s) and/or copyright holder(s), unless the work is under an open content license (like Creative Commons).

Take-down policy
If you believe that this document breaches copyright please contact us providing details, and we will remove access to the work immediately and investigate your claim.

Downloaded from the University of Groningen/UMCG research database (Pure): http://www.rug.nl/research/portal. For technical reasons the number of authors shown on this cover page is limited to 10 maximum.

Download date: 20-09-2021

VIII RUMBLING WIND: wind induced sound in a screened microphone

VIII.1 Overview of microphone noise research

It is commonly known that a wind screen over a microphone reduces 'wind noise' that apparently results from the air flow around the microphone. An explanation for this phenomenon has been addressed by several authors. According to a dimensional analysis by Strasberg [1988] the pressure within a spherical or cylindrical wind screen with diameter D in a flow with velocity V, depends on Strouhal number Sr = fD/V, Reynolds number Re = DV/ν and Mach number M = V/c (where ν is the kinematic viscosity of air and c the velocity of sound). Writing the rms pressure in a relatively narrow frequency band centered at frequency f as p_f, and in dimensionless form by division with ρV^2, Strasberg found: $p_f/\rho V^2 = function(\mathrm{Sr}, \mathrm{Re}, \mathrm{M})$. Comparison with measured 1/3 octave band levels from four authors on 2.5 - 25 cm diameter wind screens, in air velocities ranging from 6 to 23 m/s yielded a definite expression for 1/3 octave frequency band:

$$20\cdot\log_{10}(p_{1/3}/\rho V^2) = -23\cdot\log_{10}(f_m D/V) - 81 \qquad \text{(VIII.1)}$$

where f_m is the middle frequency of the 1/3 octave band. The data points agreed within appr. 3 dB with equation VIII.1 for $0.1 < fD/V < 5$, except for one of the fourteen data series where measured values diverged at $fD/V > 2$. Equation VIII.1 can also be written in acoustical terms by expressing the rms pressure as a sound pressure level relative to 20 μPa:

$$L_{1/3} = 40\cdot\log_{10}(V/V_o) - 23\cdot\log_{10}(f_m D/V) + 15 \qquad \text{(VIII.2)}$$

Here V_o is a reference velocity of 1 m/s and $\rho = 1.23$ kg/m^3 is used (air density at 1 bar and 10 °C). Equation VIII.2 is slightly different from the expression given by Strasberg because SI-units are used and terms in logarithms have been non-dimensionalized.

Morgan and Raspet pointed out that all measurements reported by Strasberg were made in low turbulence flows, such as wind tunnel flow [Morgan *et al* 1992]. Strasberg's result thus referred to the wake created by a wind screen and excluded atmospheric turbulence (as Strasberg had

noted himself in his concluding remarks [Strasberg 1988]). Outdoors, however, the flow is turbulent, and induced pressure variations are expected to depend on meteorological parameters also. Morgan & Raspet applied Bernoulli's principle by decomposing the wind velocity U in a constant time-averaged velocity V and a fluctuation velocity u with a time average u = 0, to obtain the rms pressure fluctuation $p = \rho V u$ [Morgan *et al* 1992] (in this chapter italics are used to denote the rms value x of a variable x: $x = \sqrt{x^2}$). This method can be compared to Strasberg's model for a microphone in turbulent water flow [Strasberg 1979]. Measurements in wind velocities of 3 – 13 m/s at 30.5 m and 1.5 m height for different screen diameters (90 and 180 mm) and screen pore sizes (10, 20, 40 and 80 ppi) yielded:

$$p = \alpha \cdot \rho (V u)^k \qquad \text{(VIII.3)}$$

with α ranging from 0.16 to 0.26 and k from 1.0 to 1.3 [Morgan *et al* 1992]. For some measurements Morgan *et al* showed spectra over almost the same frequency range where equation VIII.1 is valid ($0.1 < fD/V < 5$). The spectra have a positive slope up to 3 Hz, possibly due to a non-linear instrumental frequency response. At higher values the slope is roughly comparable to what Strasberg found, but values of $20 \cdot \log_{10}(p_{1/3}/\rho V^2)$ are generally 8 – 20 dB higher as predicted by equation VIII.1, implying that atmospheric turbulence dominated expected wake turbulence.

Zheng and Tan tried to solve this problem analytically [Zheng *et al* 2003]. Their analysis applies to low frequency variations, so the velocity variation u is uniform over the wind screen. Zheng & Tan state that this assumption seems to be valid for a low screen number D/λ (< 0.3), the ratio between screen diameter and wavelength. Ignoring viscous effects (*i.e.* infinite Reynolds number), and calculating the pressure variation p(0) at the center of a spherical wind screen caused by pressure variations at the surface induced by a wind velocity U = V + u, they found $p(0) = -\frac{1}{2} \cdot \rho V u$ or:

$$p(0) = \tfrac{1}{2} \rho V u \qquad \text{(VIII.4)}$$

Comparison with equation VIII.3 shows that now α = 0.5 and k = 1.

Finally, in this overview, Boersma [1997] found that sound spectra due to wind measured at 1.5 m above flat, open grassland were in good agreement with Strasberg's results. However, Boersma used 95 percentile levels (L_{95}) which he estimated to be 6 to 13 dB lower than equivalent sound levels in the range considered ($30 < L_{95} < 70$ dB) [Boersma 1997], but he did not apply a level correction. So, in fact he found that his wind related spectra had slopes comparable to Strasberg's, but with a 6 – 13 dB higher value, not unlike the Morgan & Raspet spectra.

So, from literature we conclude that air turbulence creates pressure fluctuations especially at low frequencies, but the origin -wake or atmospheric turbulence- has not been definitely resolved.

In this chapter we will try to estimate the level of pressure variations due to atmospheric turbulence, *i.e.* the 'sound' pressure level taken from a sound level meter caused by turbulence on the microphone wind screen. First we will describe the spectral distribution of atmospheric turbulence and the effect this turbulence has on a screened microphone. Then we will turn to measured spectra related to wind, obtained by the author as well as by others. Finally the results will be discussed.

VIII.2 Atmospheric turbulence

A wind borne eddy that is large relative to the microphone wind screen (hence the change of wind velocity is nearly the same all over the wind screen) can be regarded as a change in magnitude and/or direction of the wind velocity [Zheng *et al* 2003]. The change in the magnitude of the velocity causes a change in pressure; the change in direction is irrelevant for a spherical wind screen as nothing changes relative to the sphere. As we saw in the previous section, when the velocity U is written as a constant (average) wind velocity V and a fluctuating part u, and similarly $P = P_{average} + p$, the relation between the rms microphone pressure fluctuation p and the rms wind velocity fluctuation u is $p = \alpha\rho V u$. For inviscid flow $\alpha = 0.5$. For finite Reynolds numbers ($Re/10^4 \approx 0.5 – 15$ for wind screens of 4 – 20 cm and wind velocities of 2 – 12 m/s), screening is better [Zheng *et al* 2003], and $\alpha \leq 0.5$; Morgan & Raspet [1992] found $\alpha = 0.16 – 0.26$. The

pressure level due to atmospheric turbulence can be expressed as a sound pressure level L_{at} (with reference pressure p_{ref} = 20 μPa):

$$L_{at}(u) = 20 \cdot \log_{10}(\alpha \rho V u / p_{ref}) \qquad \text{(VIII.5)}$$

which is frequency dependent because of *u*.

VIII.2.1 Turbulence spectra

Turbulent velocity fluctuations v and w also exist perpendicular to the average wind velocity, in the vertical (w) as well as horizontal (v) direction, and are of the same order of magnitude as in the longitudinal direction [Jensen *et al* 1982]. Zheng & Tan [2003] showed that the effect of these fluctuations on the pressure at the microphone can be neglected in a first order approximation, as it scales with v^2 and w^2 and is therefore second order compared to the effect of the component u in line with the average wind velocity V that scales as Vu.

Atmospheric turbulence is treated in many papers and textbooks (such as [Jensen *et al* 1982, Zhang *et al* 2001]), also in reference to acoustics (see, *e.g.*, [Wilson *et al* 1994]). Here a short elucidation will be presented, leading to our topic of interest: turbulence spectra.
Atmospheric turbulence is created by friction and by thermal convection. Turbulence due to friction is a result of wind shear: at the surface the wind velocity is zero whereas at high altitudes the geostrophic wind is not influenced by the surface but a result of large scale pressure differences as well as Coriolis forces resulting from earth's rotation. In between, in the atmospheric boundary layer wind velocity increases with height z, equation III.2 is valid and for convenience repeated here :

$$V = (u_* / \kappa) \cdot [\ln(z/z_o) - \Psi] \qquad \text{(VIII.6)}$$

For $-1 < \zeta < 1$, $\Psi(\zeta)$ is of the same order of magnitude as the logarithmic term in equation VIII.6 ($2 < \ln(z/z_o) < 6$ for $1 < z < 5$ m, $1 < z_o < 10$ cm). Hence, at the same height and roughness length, V may still change appreciably due to (in)stability.

The friction created by wind shear produces eddies over a range of frequencies and lengths, their size determined by z and V. These eddies break up in ever smaller eddies and kinetic turbulent energy is cascaded to smaller sizes at higher frequencies, until the eddies reach the Kolmogorov size η_s ($\approx$ 1 mm) and dissipate into heat by viscous friction. It has been shown by Kolmogorov that for this energy cascade, in the so-called inertial subrange of the turbulent spectrum, the frequency dependency follows the well known 'law of 5/3': the spectrum falls with $f^{-5/3}$.
It is customary in atmospheric physics to express turbulence frequency in dimensionless form n, with $n = fz/V$ (in fact n and f are usually interchanged, but we will use f for dimensional frequency, as is usual in acoustics). The seminal Kansas measurements showed that the squared longitudinal velocity fluctuation u_f^2 per unit frequency in a neutral atmosphere depends on frequency as [Kaimal *et al* 1972]:

$$f \cdot u_f^2 / u_*^2 = 105n \cdot (1+33n)^{-5/3} \qquad \text{(VIII.7)}$$

The experimentally determined constants in this equation, the non-dimensional turbulent energy spectrum, are not exact, but are close to values determined by others [Garrat 1992, Zhang *et al* 2001]. For $n << 1$, the right-hand side approximates 105n, which, with $n = fz/V$ and equation VIII.6, leads to $u_f^2 = 105 \cdot u_*^2 \cdot z/V = 105\kappa^2 zV \cdot [\ln(z/z_o) - \Psi]^{-2}$. Applying this to VIII.5, the induced pressure level per unit of frequency appears to be independent of frequency, but increases with wind velocity (~ 30·logV).
For $n >> 1$ the right-hand side of equation VIII.7 reduces to $3.2 \cdot (33n)^{-2/3}$, leading to $u_f^2 = 0.3 \cdot u_*^2 \cdot (V/z)^{2/3} \cdot f^{-5/3}$, which describes the inertial subrange. The frequency where the wind velocity spectrum VIII.7 has a maximum is $n_{max} = 0.05$ or $f_{max} = 0.05V/z$. As sound measurement are usually at heights $1 < z < 5$ m, f_{max} is less than 1 Hz for wind velocities $V < 20$ m/s,

When insolation increases the surface temperature, the atmosphere changes from neutral to unstable and eddies are created by thermal differences with sizes up to the boundary layer height with an order of magnitude of 1 km. Turbulent kinetic energy production then shifts to lower frequencies. In contrast in a stable atmosphere, where surface temperature decreases because of surface cooling, eddy production at low frequencies

(corresponding to large eddy diameters) is damped and the spectral maximum shifts to a higher frequency up to appr. n = 0.5 for a very stable atmosphere. As low-altitude wind velocities (z < 5 m) in a stable atmosphere are restricted to relatively low values (for higher wind velocities, stability is disrupted and the atmosphere becomes neutral), the spectral maximum may shift up to 0.5V/z ≈ 3 Hz. The inertial subrange thus expands or shrinks at its lower boundary, but its frequency dependency follows the 'law of 5/3'.

VIII.2.2 Effect on microphone in wind screen

The spectrum of longitudinal atmospheric turbulence in the inertial subrange was described in the previous section with the (squared) rms value of velocity variation per unit frequency $u_f^2 = 0.3 \cdot u_*^2 \cdot (V/z)^{2/3} \cdot f^{-5/3}$. It is convenient to integrate this over a frequency range f_1 - f_2 to obtain a 1/3-octave band level ($f_m = 2^{-1/6} \cdot f_2 = 2^{1/6} \cdot f_1$) with centre frequency f_m: $u_{1/3}^2 = 0.046 \cdot u_*^2 \cdot (f_m \cdot z/V)^{-2/3} = [0.215 \cdot u_* \cdot (f_m \cdot z/V)^{-1/3}]^2$. Substituting u_* from equation VIII.6 and applying the result to equation VIII.5 for 1/3 octave band levels $L_{at,1/3}(f_m) = 20 \cdot \log(\alpha \rho V u_{1/3}/p_{ref})$, yields:

$$L_{at,1/3}(f) = 40 \cdot \log(V/V_o) - 6.67 \cdot \log(zf/V) - 20 \cdot \log[\ln(z/z_o) - \Psi] + C \quad \text{(VIII.8)}$$

Here the frequency index m as well as the logarithm index 10 have been dropped, as will be done in the rest of the text. In equation VIII.8 $C = 20 \cdot \log(0.215 \kappa \alpha \rho V_o^2/p_{ref}) = 62.4$ dB for $\kappa = 0.4$, $\alpha = 0{,}25$, $\rho = 1{,}23$ kg/m^3 and pressure level is taken re $p_{ref} = 20$ μPa. For octave band levels $L_{at,1/1}(f)$ the constant C in the right hand side of VIII.8 is 67.2 dB.

Equation VIII.7 does not apply to frequencies where eddies are smaller then the wind screen. The contribution of small eddies will decrease proportional to the ratio of eddy size (ℓ^2, where ℓ is the eddy length scale and $f = V/\ell$) and wind screen surface πD^2. When this ratio decreases more eddies will simultaneously be present at the screen surface and resulting pressure fluctuations at the surface will more effectively cancel one another in the interior of the wind screen. The pressure variation in the wind screen centre resulting from one eddy is proportional to the size of

the eddy relative to the screen surface, *i.e.* ℓ^2/D^2, but also the screen centre pressure resulting from the random contributions of all N eddies on the screen surface is proportional to $\sqrt{N}$, where $N \sim D^2/\ell^2$. The resulting screen centre pressure is thus proportional to individual eddy pressure p_f and $(\ell^2/D^2)\cdot\sqrt{(D^2/\ell^2)} = \ell/D = V/fD$. Consequently a factor $-20\cdot\log(fD/V)$ must be added to the resulting rms pressure level.

In wind noise reduction measured by Morgan there is a change in frequency dependency at screen number $D/\ell \approx 1/3$ ([Morgan 1993], see also [Zheng *et al* 2003]). We therefore expect at sufficiently high frequencies the pressure level at the microphone to decrease proportional to $20\cdot\log(D/\ell)$, relative to the level in equation (VIII.8), and this decrease must vanish when $D/\ell = Df/V < 1/3$, *i.e.* below the cut-off frequency $f_c = V/(3D)$. As the change will be gradual, a smooth transition can be added to equation VIII.8:

$$L_{at,1/3}(f) = 40\cdot\log(V/V_o) - 6.67\cdot\log(zf/V) - 20\cdot\log[\ln(z/z_o)-\Psi] + \\ - 10\cdot\log(1+(f/f_c)^2) + C \qquad \text{(VIII.9a)}$$

With usual screen diameters 5 – 25 cm and wind velocities 1 - 20 m/s, the cut-off frequency is in the range of 1 to 100 Hz. With the common 10 cm diameter wind screen f_c will usually be in the infrasound region. Equation VIII.9a can be rewritten with Strouhal number $Sr = fD/V$ as independent variable of a 'meteorologically reduced' 1/3 octave band level L_{red}:

$$L_{red,1/3} = L_{at,1/3} - 40\cdot\log(V/V_o) + 20\cdot\log[(z/D)^{1/3}\cdot(\ln(z/z_o)-\Psi)] = \\ - 6.67\cdot\log(Sr) - 10\cdot\log[1+ (3Sr)^2] + C \qquad \text{(VIII.9b)}$$

The levels according to equation VIII.9 have been plotted in figure VIII.1 for different wind velocities and with $z = 20\cdot D = 40\cdot z_o = 2$ m, $\Psi = 0$. For $f < 0.5\cdot f_c$ the term before C is less then 1 dB and equation VIII.9a reduces to equation VIII.8. For frequencies $f >> f_c$ the term before C in equation VIII.9b reduces to $-20\cdot\log(3Sr)$ and equation VIII.9b can be written as:

$$L_{red,1/3} = - 26.67\cdot\log(Sr) + C - 9.5 \qquad \text{(VIII.10a)}$$

This can be rewritten in a aerodynamic terms as:

$L_{p,1/3} = 20\cdot\log(p_{1/3}/\rho V^2) = -26.67\cdot\log(Sr) + F(z) + C_p$ (VIII.10b)

where and $F(z) = -20\cdot\log[(z/D)^{1/3}\cdot(\ln(z/z_o)-\Psi)$ and $C_p = 20\cdot\log(0.215\kappa\alpha) - 9.5 = -43$ dB. For F(z) = -20 dB (*e.g.* a 10 cm diameter wind screen at a z = 2 m, z_o = 5 cm and Ψ = 0) the right hand side of equation VIII.10b is $-26.67\cdot\log(Sr) - 63$. Comparing this with Strasberg's result (equation VIII.1 and gray lines in figure VIII.1) we see that the frequency dependency is slightly different, and levels are 13 - 19 dB higher ($0.5 < Sr < 20$), which is of the order of what we found in the measurements by Boersma and Raspet *et al* (see section VIII.1). The change in slope, visible at Strouhal number $Df_c/V = 1/3$ in figure VIII.1, is a feature not explained by the earlier authors.

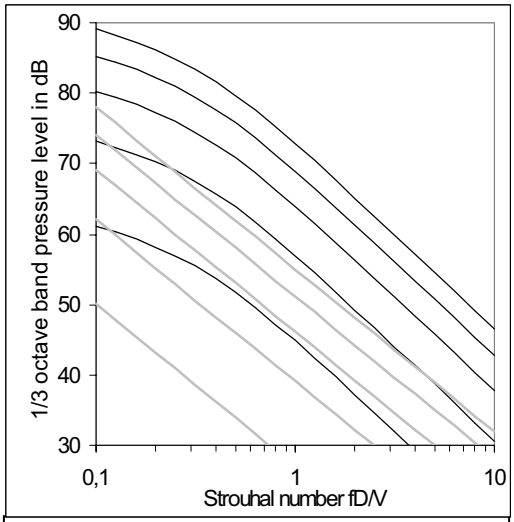

Figure VIII.1: black lines: calculated 1/3 octave band levels $L_{at,1/3}$ due to atmospheric turbulence at wind velocities of (bottom to top) 2, 4, 6, 8 and 10 m/s; F(z) = -18 dB; gray lines: levels at same wind velocities according to Strasberg

VIII.2.3 Frequency regions

From the theory above it can now be concluded that the wind induced pressure level on a (screened) microphone stretches over four successive frequency regions:

i. at very low frequencies (less than a few Hz) the turbulence spectrum is in the energy-producing subrange; 1/3 octave band pressure level $L_{at,1/3}$ is independent of frequency (white noise), but increases with wind velocity;
ii. at frequencies up to f_c = 0.3V/D, which is usually in the infrasound region, the turbulence spectrum is in the inertial subrange, $L_{at,1/3} \sim 46.7\cdot\log V$ and $\sim -6.7\cdot\log f$;
iii. at higher frequencies, but still in the inertial subrange, eddies average out over the wind screen more effectively at increasing frequency

($L_{at,1/3} \sim -26.7 \cdot \log f$), but pressure level increases faster with wind velocity ($L_{at,1/3} \sim 66.7 \cdot \log V$) ;

iv. at frequencies beyond $0.1V/\eta_s$ (see [Plate 2000, p. 585]) atmospheric turbulence enters the dissipation range and turbulence vanishes. This is in the range $Sr = fD/V > 0.1D/\eta_s \approx 100 \cdot [D/\text{m}] = D/\text{cm}$.

The inertial subrange (ii and iii) is of most interest here, as it is within the commonly used range of acoustic frequency and level.

VIII.2.4 Wind induced broad band A-weighted pressure level

In figure VIII.2 1/3-octave band levels according to equation VIII.9 are plotted for different wind velocities for $z = 50 \cdot z_o = 20 \cdot D = 2$ m (or F(z) = -20.5 dB with $\Psi = 0$). Also levels are plotted after A-weighting to show the relevance to most acoustic measurements, where wind induced noise may be a disturbance added to an A-weighted sound level. At the frequency where turbulent eddies enter the dissipation subrange ($f \approx 0.1V/\eta_s$), no data are plotted as the turbulent velocity spectrum falls very steeply and induced pressure levels are considered negligible. A-weighted pressure levels $L_{at,A}$ can be calculated by summing over all 1/3-octave bands. The wind velocity dependency can then be determined from the best fit of $L_{at,A}$ vs. V:

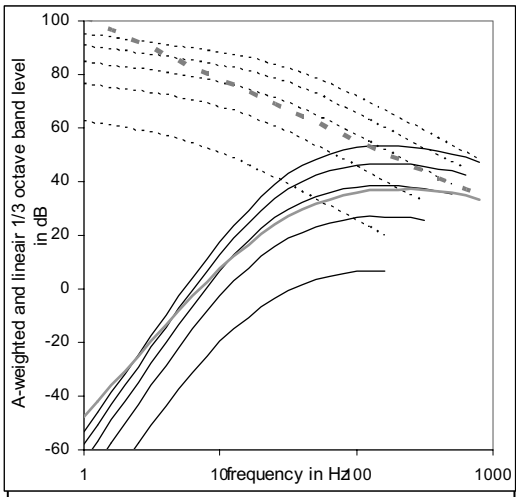

Figure VIII.2: calculated lineair (dashed) and A-weighted (solid lines) 1/3-octave pressure levels due to atmospheric turbulence on a screened microphone with F(z)+C=42 dB, D = 0.1 m and wind speeds 2, 4, 6, 8, 10 m/s (black, bottom to top); bold grey lines: 1/3 octave band levels according to Strasberg for 10 m/s

$$L_{at,A} = 69{,}4 \cdot \log(V/V_o) - 26.7 \cdot \log(D/\ell_o) + F(z) + C - 74.8 \qquad \text{(VIII.11a)}$$

where ℓ_o = 1 m is a reference length. Equation VIII.11a has the same structure as VIII.10a, but a rather higher slope with logV because higher frequencies (with lower A-weighting) are progressively important, and a much smaller constant term as a result of A-weighting. The slope decreases with wind screen diameter and is 65.5 dB when D = 1.25 cm (unscreened ½“ microphone), but is constant within 1 dB for 5 < D/cm < 50. Equation VIII.11a is not very sensitive for the cut-off at $f = 0.1V/\eta$: if spectral levels are integrated over all frequencies, total level does not increase significantly at high wind velocities, and with less than 3 dB at low wind velocities. It will be noted that the slope with wind velocity is slightly higher than for individual spectral levels for $f > fc$ (66.7 dB, see equation VIII.10a, due to lower A-weighting at the increasingly higher frequencies.
If we put $G(z) = F(z) - 6.7\cdot\log(D/\ell_o) + 14 = -20\cdot\log[0.2\cdot(z/\ell_o)^{1/3}\cdot(\ln(z/z_o - \Psi)]$, and use 10D for convenience, equation VIII.11a becomes:

$$L_{at,A} = 69.4\cdot\log(V/V_o) - 20\cdot\log(10D/\ell_o) + G(z) + C - 68.8 \qquad \text{(VIII.11b)}$$

Now for z_o = 2,5 - 6 cm and $\Psi = 0$, G(2 m) = 0 ± 1 dB. This means that for a 10 cm wind screen and measurement over a flat area with a low vegetation cover in neutral conditions $L_{at,A} \approx 69.4\cdot\log(V/V_o) - 6.4$ dB(A).
Figure VIII.3 is a plot of equation VIII.11 with G(z) = 0, C = 62 dB. Also plotted in figure VIII.3 is the relation according to Strasberg, obtained by A-weighting and integrating equation VIII.2 over *f*.

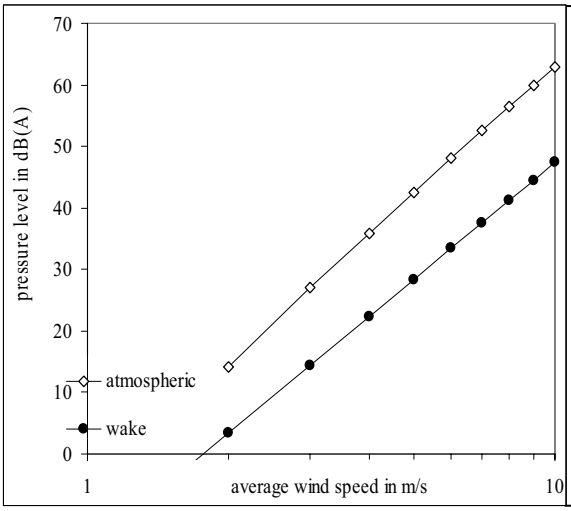

Figure VIII.3: calculated A-weighted broad band pressure level caused by atmospheric or wake turbulence with G(z)+C = 62.4 dB and D = 0.1 m

VIII.3 Comparison with experimental results

VIII.3.1 Measured spectral pressure levels

Several authors have performed measurements to determine spectral levels due to wind, including wind induced sound pressure fluctuations. We will use data from Larsson and Israelsson [1982], Jakobsen and Andersen [1983] and Boersma [1997] from screened as well as unscreened microphones. Table VIII.1 gives an overview of measurement parameters. None of the authors give the degree of stability, but in Jakobsen's data $\Psi \leq 0$ (night), in Boersma's $\Psi \geq 0$ (summer's day). Jakobsen mentions roughness height of the location (a golf course), Boersma grass height ($\approx$ 10 cm), Larsson only mentions measurement height over grass at either 1.25 or 4 m, without specifying which height applies to a measurement result. To prevent using spectra at large values of $|\Psi|$ no data at low wind velocities (< 2 m/s at microphone) are used. This is also recommendable as at low wind velocity sound not related to wind is more likely to dominate. We preferably use L_{eq} data. However, these are not available from Boersma. Boersma used 95 percentile levels (L_{95}), but we have L_{50} values from the original data. Though Boersma quotes $L_{Aeq} \approx L_{A50}$, we will use $L_{Aeq} \approx L_{A50} + 3$, in agreement with long term data on wind noise [Van den Berg 2004b] and assume this to be valid for every frequency band. If measurements yielded octave band levels, 4.8 dB was subtracted to obtain the 1/3 octave band level at the same frequency.

Also L_{eq} values are presented from measurements made by the author at several locations; at one location (Zernike) for the purpose of wind noise measurements, and otherwise (Horsterwold, Kwelder) selected for having little other noise. Here also the degree of atmospheric stability is unknown, as at the time of measurement it was not known to be a relevant factor. The 'Zernike' measurements were done at the university grounds (latitude 53°14'43", longitude 6°31'48") with both the microphone (in a spherical foam screen of 2.5, 3.8 or 9.5 cm diameter) and the wind meter at 1.2 or 2.5 m over grass at least several hundred meters from trees, and an estimated roughness height of 5 cm. They were performed in daytime in December 2003 and august 2004 with a fair wind under heavy clouding.

The ‘Kwelder’ measurements were made in daytime or evening in July and August of 1996 at an open area at the Dutch coast (latitude 53°25’46”, longitude 6°32’40”), consisting of level land overgrown with grass and low weeds and close to tidal water. Sound measurements were taken at a height of 1.5 m at times when no sound could be heard but wind-related sound and distant birds. The microphone was fitted with a spherical 9.5 cm diameter foam wind screen. Wind velocity at microphone height at 1.5 m was estimated from measured wind velocity at 5 m height with equation VIII.6, z_o estimated as 2 cm. Finally the ‘Horsterwold’ measurements were made in December 2001 in an open space with grass and reeds (latitude 52°18’3”, longitude 5°29’38”) between 5 to 10 m high trees at a distance of approximately 30 m but further in the windward direction, in a mostly clouded night. Wind velocity and sound were measured at 2 m height, the wind screen was a 9 cm diameter foam cylinder. Due to the differences in vegetation, roughness length here was difficult to estimate, and was determined by fitting measurement results to the expected level (resulting in 60 cm and a more limited range of values of Ψ to fit).

At very low frequencies in our Zernike measurements the 1/3 octave band levels were corrected for non-linear response. The frequency response of the B&K ½" microphone type 4189 is specified by Brüel & Kjaer [B&K 1995] and is effectively a high pass filter with a corner frequency of 2.6 Hz. The response of the Larson Davis type 2800 frequency analyser is flat (±1 dB) for all frequencies.
To plot spectra we calculate the reduced pressure level $L_{red,1/3}$, leaving only the screen diameter based Strouhal number $Sr = fD/V$ as the independent variable. Octave band pressure levels $L_{red,1/1}$ are substituted by $L_{red,1/3} + 4.8$. As atmospheric stability is as yet unknown, the stability function is set to zero. If wind velocity was not measured at microphone height, the logarithmic wind profile (equation (VIII.6 with $\Psi = 0$, or III.3) is used to determine V_{mic} from the wind velocity at height h.

Linear spectra of 1/3-octave levels are plotted in the left part of figure VIII.4 for the unscreened microphones. Also plotted is the spectrum according to Larsson *et al* [1982], valid for the inertial subrange. Due to

the small size of the unscreened microphone (1.25 cm) part of the spectrum lies in the dissipation range at frequencies $f > 0.1V/\eta \approx 100V/m$, corresponding to Sr > 100D/m = 1.25.
In figure VIII.4B spectra are plotted from screened microphones, from the data from Larsson, Jakobsen and Boersma. As these spectra were determined with a range of screen diameters, the change from the inertial to the dissipation subrange extends over a range of non-dimensional frequencies (Strouhal numbers). Finally figure VIII.4C shows spectra from the Horsterwold, Zernike and Kwelder measurements. In all figures spectra deviate from the predicted spectrum at high Strouhal numbers because either the lower measurement range of the sound level meter is reached or

Table VIII.1: wind induced noise measurement characteristics

author	period	location	zo (cm)	H_{wind} (m)	H_{mic} (m)	V_{mic} (m/s)	D (cm)	T (min.)	N [1]	F (Hz)	band width [6]
Larsson *et al*	late summer - early autumn	grass lawn	5 [2]	mic	1.25 or 4	2 – 7	no [4] 9.5	6 obs. [5]	9 9	63-8k	1/1
Jakobsen *et al*	summer – dec, night	golf course	2	10	1.5	3 – 7	9.5 / 25	? [5]	5 / 5	63-8k	1/1
Boersma	summer, day	grass land	3 [2]	2	1.5	3 – 7 2 – 9	no [4] 9	160 430	9 7	6-16k 6-16k	1/3
this study:											
Horster-wold	night, clouded	grass, reeds	60 [3]	10	2	4 - 6	9.5	230	4	31-8k	1/1
Kwelder	summer, day	grass, herbs	2 [2]	5	1.5	3 - 5	9.5	40	6	6-16k	1/3
Zernike	summer, clouded day	grass land	5 [2]	1.5	2.5	5	2.5/3.8 /9.5	30	3	6-1k	1/3
	winter, clouded day				1.2	4	3.8/9.5	20	2	1-1k	

notes: 1: # of measurements 2: estimated; 3: fitted; 4: no = unscreened;
5: observations of unknown length; 6: 1/1 or 1/3 octave band

Figure VIII.4:
reduced 1/3 octave band pressure levels at different wind velocities (in legend: V in m/s), bold line is predicted spectrum;

A: unscreened microphone, from Larsson (open symbols) and Boersma (black symbols);

B: screened microphone, from Larsson (open symbols), Jakobsen (grey) and Boersma (black symbols);

C: screened microphone, measurements in Horsterwold (open symbols), Kwelder (grey) and Zernike (black symbols).

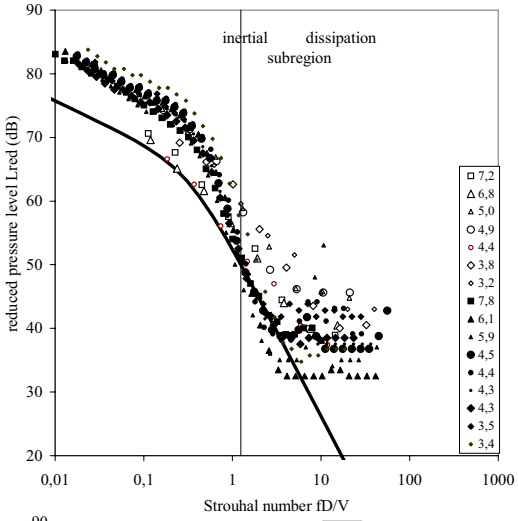

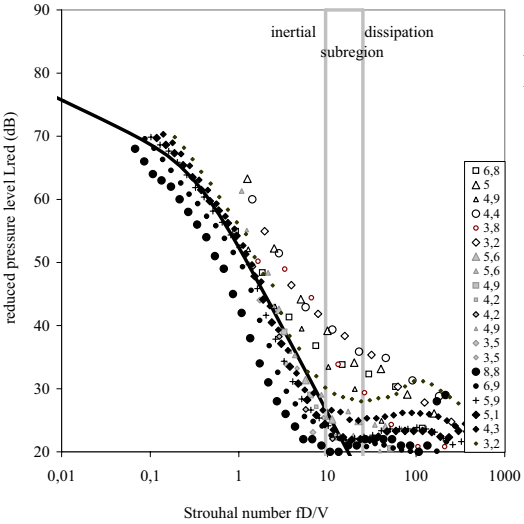

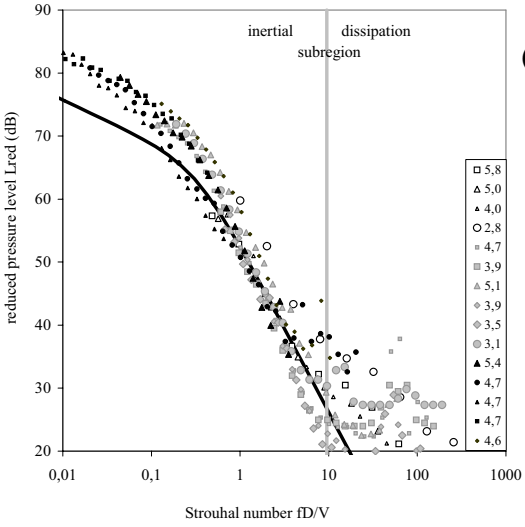

A

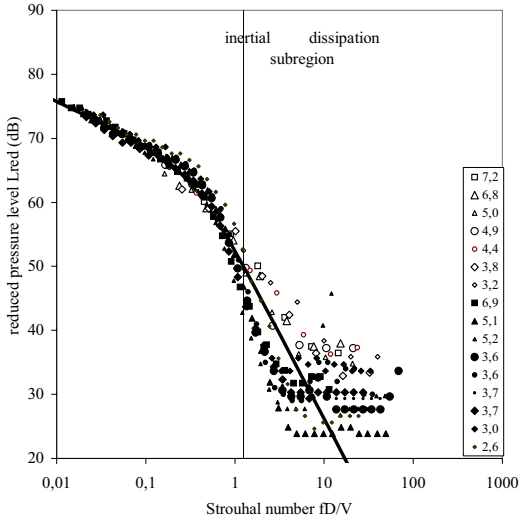

B

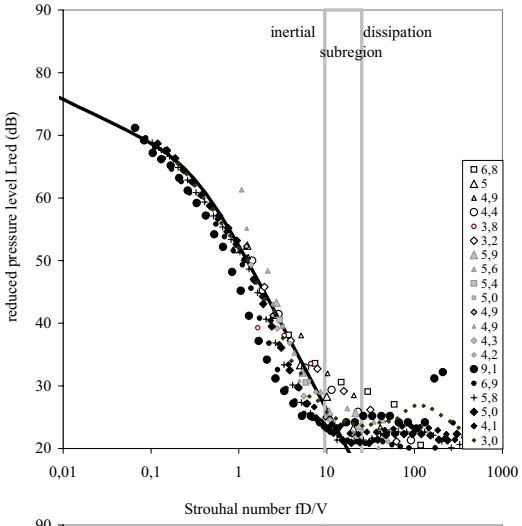

C

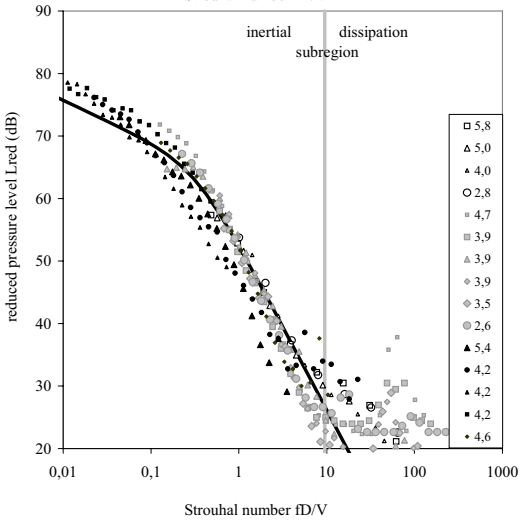

Figure VIII.5:
same as figure VIII.4, but after fitting with stability function

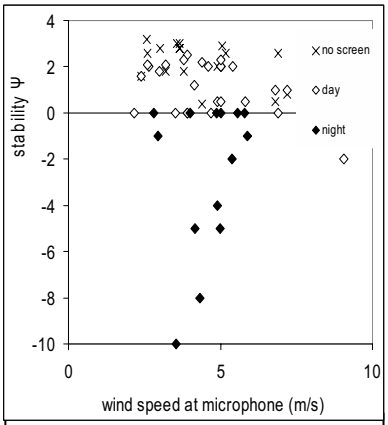

Figure VIII.6: values of the stability function Ψ found by fitting reduced spectral levels L_{red} with theoretical spectrum, for measurements in day or night time, and for unscreened microphones in daytime

ambient sound dominates the wind-induced pressure level. Also, at these high Strouhal numbers most values are in the dissipation range where the present model is not valid.

In figure VIII.4 atmospheric stability has not been taken into account yet (in fact $\Psi = 0$ was used), due to lack of data to determine Ψ. In stable conditions ($\Psi < 0$) L_{red} will be higher, in unstable conditions ($\Psi > 0$) lower, causing the plotted spectra to shift vertically if the proper value $\Psi \neq 0$ is applied.
If wind velocity at microphone height is deduced from wind velocity at another height, the shift is more complex, as stability then also affects the term $40 \cdot \log(V/V_o)$ as well as the ordinate value $Sr = fD/V$. The approach taken here is to vary Ψ to obtain a best fit to the theoretical value of the L_{red} levels at non-dimensional frequencies in the inertial subrange. The fitted spectra are plotted in figure VIII.5. The values of Ψ that gave the best fits are plotted in figure VIII.6, categorized in daytime and night time measurements (where one would expect $\Psi \geq 0$ and $\Psi \leq 0$, respectively). Measurements with unscreened microphones are indicated separately, and are in daytime for Boersma's measurements and probably also for Larsson's, so one would expect $\Psi \geq 0$.

VIII.3.2 Measured broad band pressure levels

Several authors give a relation between broad band A-weighted sound pressure level L_A and wind velocity [Boersma 1997, Larsson *et al* 1982, Jakobsen *et al* 1983]. According to Boersma $L_A \sim 22.6 \cdot \log(v)$ (with v measured at 2 m height, L_A at 1.5 m), to Larsson $L_A = 4.4 \cdot v + 27.5$ (v and L_A measured at the same height), to Jakobsen $L_A = 6.8 \cdot v - 2.6$ (v measured at 10 m, L_A at 1.5 m). However, as Boersma clearly shows, most of the A-weighted sound is due to ambient wind induced sound, especially at low wind velocities. So we cannot use these relations for just sound induced by wind on the microphone.

A practical situation where the influence of wind on the microphone + wind screen could be investigated directly offered itself when on May 28, 2000 a storm occurred during our 'Wieringerwaard' measurements. The

microphone, in a 9 cm foam cylinder, and a wind meter were both placed at a height of 4.6 m, 2 m apart, in front of a big farmer's shed 5 m to the west of the microphone (latitude 52°48’41”, longitude 4°52’23”). A second, 'free wind' windmeter at 10 m height was placed further away to measure undisturbed wind. Around the measurement location were fields with potato plants of 20 - 30 cm height. As it was May, an unstable atmosphere is expected in daytime, leaning to neutral when the wind velocity increases.

Some measurement results are given in figure VIII.7 (all values are 10 minute averages of samples measured at a rate of 1 s^{-1}). In the left part of the figure the 'free' wind velocity v_{10} is seen to increase to 20 m/s (72 km/h) in the course of the day after a relatively quiet night. The wind velocity v_{mic} near the microphone increased at practically the same rate between 6 and 12 o'clock, but then abruptly falls from 13 m/s to 2 m/s and thereafter remains at a low value even while the 'free' wind velocity is still increasing. Up to 12 o'clock the sound level (equivalent A-weighted level per 10 minutes) increases in proportion to the wind velocity reaching a maximum of 84 dB(A), but then falls abruptly to 50 dB(A) at the same time the local wind velocity collapses. In this morning the unobstructed wind began in the east and gradually turns south. When at 12 o’clock the wind passes behind the shed, the microphone is suddenly taken out of the wind. There is no reason that the *sound* reaching the microphone changes significantly during this change, but due to the sudden wind velocity reduction the measure sound pressure level drops to 50 dB(A). After that the sound pressure level increases again as long as the storm is gaining strength. The measured pressure level above 60 dB(A) is pure wind-induced ‘pseudo’ sound, that is: sound resulting from moving air, not from airborne sound.

In the right part of figure VIII.7 the A-weighted equivalent (pseudo-) sound pressure level per 10 minutes over the same period as in the left part of figure 7, is plotted as a function of wind velocity at the microphone. There is an obvious direct correlation between pressure level and wind velocity at higher wind velocities ($V \geq 6$ m/s) in contrast to the levels at

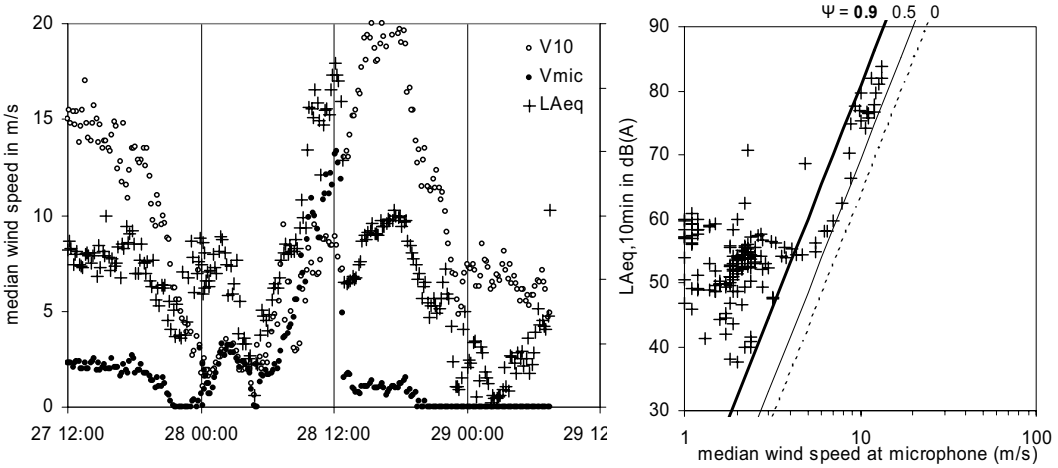

Figure VIII.7: measurements during a storm in front of a big shed; left: 10 minute averages of wind speed at microphone and at 10 m height and sound pressure level Leq; right: Leq as a function of microphone wind speed and predicted sound pressure level (G(4.6) = 8.2 dB)

lower wind velocities. Again, the stability factor Ψ is not known, but in daytime and in strong winds it must be small and positive. The lines in figure VIII.7 show the calculated pressure levels for plausible values $0 < \Psi < 1$ (with $z_o = 20$ cm), encompassing the measured values.

VIII.3.3 Screen reduction

For two of our Zernike summer measurements (see table VIII.1) with place and atmospheric conditions unchanged within the measurement period, the difference between 1/3 octave band pressure levels measured with an approximately spherical 2.4 cm wind screen and a spherical 9.5 cm wind screen are plotted in figure VIII.8. Also

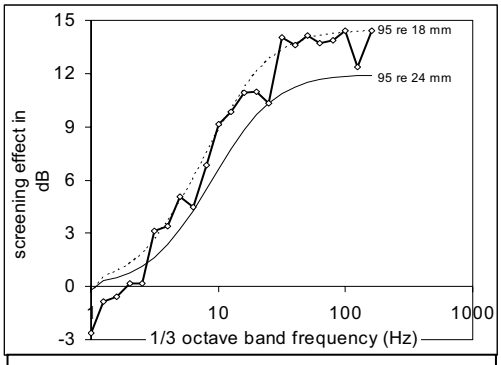

Figure VIII.8: measured (line with markers) and calculated screening effect of a 9.5 cm relative to a 2.4 or 1.8 cm wind screen

plotted is the calculated screening effect based on equation VIII.9a, with only both term before C differing between both measurements. It appears that the measured screening effect is on average approximately 1 dB higher than the calculated level. It is not clear why the difference in screening is negative at frequencies below 2 Hz. For a somewhat smaller wind screen (18 mm < D < 24 mm) the average screening effect would agree better with the calculated effect.

VIII.4 Discussion

The model developed in this paper starts with the assumption that wind induced 'sound' pressure levels on a microphone are caused by atmospheric turbulence. Then, at low non-dimensional frequencies (Sr << 0.3) spectral levels are determined entirely by atmospheric turbulence. In this frequency range a wind screen has no effect. At higher frequencies, where pressure fluctuations tend to cancel one another more effectively as their scale decreases relative to the wind screen diameter, a wind screen acts as a first order low pass filter for turbulent fluctuations. In this frequency range (Sr > 0.3) a wind screen diminishes the effect of turbulence, and better so if it is bigger.

Wind induced pressure levels are determined not just by wind velocity and screen diameter, but also by two factors that are relevant for the production of turbulence: atmospheric instability and surface roughness. The stability factor Ψ and roughness height z_o are determinants for thermal and frictional turbulence, respectively. These determinants are usually not taken into account with respect to wind induced noise and are consequently not reported. Atmospheric stability therefore had to be estimated by varying the value of Ψ until a best fit was obtained of measured spectra to the calculated spectrum. Roughness length, when unknown, was assumed to be comparable to vegetation height.

The values of Ψ that resulted in the best fits are shown in figure VIII.6. They can also be compared to values obtained from long term measurements at the Cabauw measurement site of the Royal Netherlands Meteorological Institute (KNMI). The Cabauw site is in open, flat land west of the central part of the Netherlands (see Chapter VI) and may be considered representative for locations in comparable terrain in the north

and central parts of the Netherlands (Boersma's and our measurements), Denmark (Jakobsen *et al*) and the Swedish Uppsala plain (Larsson *et al*). The KNMI provided us with a data file containing 30 minute averages of the Monin-Obukhov length L over one year (1987). From this the dimensionless height $\zeta = z/L$ can be calculated and then the stability factor Ψ (see text below equation VIII.6). In figure VIII.9 the frequency distribution is shown of all 17520 (= 2·24·365) values of Ψ, for two altitudes: 2 m and 5 m. Also the frequency distribution is shown of the 42 values of Ψ resulting from our fitting procedure. The distribution of our fitted values resemble the distribution of actually occurring values (in 1987) and thus seems plausible.

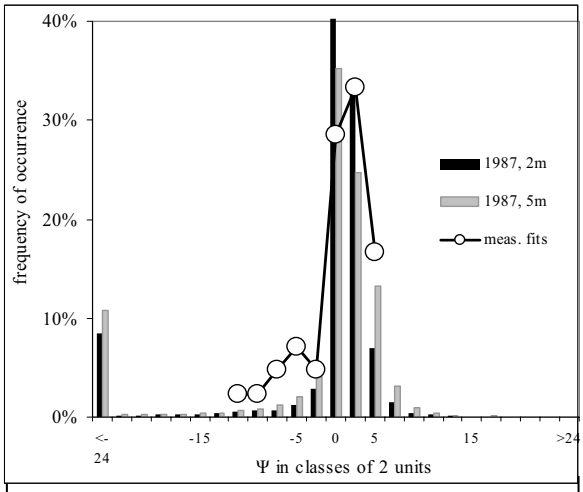

Figure VIII.9: frequency distributions of stability factor Ψ at 2m and 5 m height, based on ½ hour observations over 1987 and resulting from fitted spectra

Two constants are not known accurately: α, assumed to have a value 0.25, and the ratio of screen diameter and eddy size at the corner frequency, where 3 was used. If the Sr-related slopes are as in equation VIII.9b, the best fit of all data points in figure VIII.5 at Sr < 2.5 is a line $L_{red,1/3} = -6.7\cdot\log(Sr) - 10\cdot\log[1+ (3.8\cdot Sr)^2] + 62.0$. This fit is within 2.2 dB of the calculated value (equation VIII.9b). It follows that the ratio ℓ/D (3.8) where screen averaging over eddies sets in may be greater than assumed (*viz.* 3), and the constant term may be somewhat smaller, which could be a result of a lower value of α than assumed (0.24 instead of 0.25.

For 2.5 < Sr < 16 the best fit is on average 2.1 dB above the calculated value. The standard deviation of the measured 1/3 Strouhal octave band levels is less than 3.5 dB at Sr < 2.5 and up to 7 dB at 2.5 < Sr < 16.

VIII.5 Applications

As microphone wind noise appears to be closely correlated to atmospheric turbulence, acoustic measurements can alternatively be used to measure turbulence spectra or turbulence strength, especially in the inertial subrange. This provides a new way to determine (*e.g.*) friction velocity or atmospheric stability. As the measured signal decreases above the corner frequency f_c = V/(3D) this frequency is best chosen high, which can be achieved with a small, bare microphone.

The present model can be used to distinguish wind induced noise from other wind related sound. An application is the measurement of wind turbine sound or (without an operating wind turbine) ambient background sound in relatively strong winds. If the measurement is on a wind exposed site it is probable that at high wind velocities wind induced noise influences or even dominates either wind turbine sound or proper ambient sound. A measured level can now be corrected for wind induced sound with a calculated wind noise level. In less exposed sites it is usually not clear in what degree the measured levels are influenced by wind induced noise. To calculate wind induced noise levels additional measurements are necessary to determine roughness height and atmospheric stability. Stability can be estimated from wind velocity measurements on two heights, using equation VIII.6. Roughness height can be estimated from tabulated values or from wind velocity measurement at two heights in a neutral atmosphere, at times when the logarithmic wind profile is valid (equation VIII.6 with $\Psi = 0$). In neutral and stable conditions wind induced noise levels are not very sensitive to errors in roughness height: with an error of a factor of 2 in z_o = 10 cm, the level changes less than 2 dB if microphone height is 3 m or more.

VIII.6 Conclusion

Measured spectra, reduced with a term for wind velocity and turbulence strength, coincide well with calculated values for unscreened as well as screened microphones in the range where the theoretical model (equation VIII.9) is valid. To test the model more thoroughly, measurements should

include a determination of roughness length and atmospheric stability, in addition to the usual measurement of wind velocity and measurement height.

The model shows that to avoid high wind induced pressure levels, measurements are best performed at low wind velocity and with a large diameter wind screen, which is common knowledge in acoustics. The overall reduction ΔL_A from a bigger wind screen relative to a smaller one is determined by the ratio of the screen diameters D_1 and D_2: $\Delta L_A = 20 \cdot \log(D_2/D_1)$ (from equation VIII.11b, D > 5 cm). A wind screen does not reduce noise from atmospheric turbulence at frequencies $f < V/(3D)$.
The model also shows that, to reduce wind induced sound, it helps to measure over a low roughness surface and at night (stable atmosphere), as both factors help to reduce turbulence, even if the (average) wind velocity on the microphone does not change. With reduced turbulence, wind induced pressure levels will finally reach the level given by Strasberg (equation VIII.1 or VIII.2), where turbulence is the result of the wake caused by the wind screen.
One might be tempted to think that a higher measurement altitude would also help to reduce wind noise (as this would make G(z) in equation VIII.11b more negative, thus reducing $L_{at,A}$). However, in practice increasing altitude will lead to higher wind velocities, especially so in a stable atmosphere, and the first term in equation VIII.11b would more then compensate the decrease in G(z). It is therefore preferable to measure at low altitude if less wind noise is desired.